Magnetic Photocatalyst for Wastewater Tertiary Treatment at Pilot Plant Scale: Disinfection and Enrofloxacin Abatement

Iván Sciscenko [1],*, Sergio Mestre [2], Javier Climent [3], Francisco Valero [3], Carlos Escudero-Oñate [4], Isabel Oller [5] and Antonio Arques [1]

[1] Departamento de Ingeniería Textil y Papelera, Universitat Politècnica de València (UPV), Plaza Ferrándiz y Carbonell s/n, 03801 Alcoy, Spain; aarques@txp.upv.es

[2] Instituto Universitario de Tecnología Cerámica/Departamento de Ingeniería Química, Universitat Jaume I, Campus Universitario Riu Sec, Av. Vicent Sos Baynat s/n, 12006 Castellón, Spain; smestre@uji.es

[3] Sociedad Fomento Agrícola Castellonense S.A. (FACSA), c/mayor, 82-84, 12001 Castellón, Spain; javier.climent@grupogimeno.com (J.C.); fvalero@facsa.com (F.V.)

[4] Institute for Energy Technology (IFE), Instituttveien 18, 2007 Kjeller, Norway; carlos.escudero@ife.no

[5] Plataforma Solar de Almería (PSA)-CIEMAT, Ctra Senés km 4, Tabernas, 04200 Almería, Spain; ioller@psa.es

* Correspondence: ivsci@txp.upv.es

Abstract: In this work, we have tested a photocatalytic material consisting of a core of SiO_2/Fe_3O_4 coated with TiO_2 (Magnox) for plausible tertiary wastewater treatment. For this, a pilot plant of 45 L equipped with an Ultraviolet light (UVC) lamp was employed to study the degradation of a model contaminant, enrofloxacin (ENR), as well as water disinfection (elimination of *Escherichia coli* and *Clostridium perfringens*). The influence of different operational conditions was explored by means of dye (rhodamine-B) decolorization rates, analyzing the effects of photocatalyst quantity, pH and recirculation flow rates. The magnox/UVC process was also compared with other four Advanced Oxidation Processes (AOPs): (i) UVC irradiation alone, (ii) hydrogen peroxide with UVC (H_2O_2/UVC), (iii) Fenton, and (iv) photo-Fenton. Although UVC irradiation was efficient enough to produce total water disinfection, only when employing the AOPs, significant degradations of ENR were observed, with photo-Fenton being the most efficient process (total enrofloxacin removal in 5 min and c.a. 80% mineralization in 120 min, at pH_0 2.8). However, Magnox/UVC has shown great pollutant abatement effectiveness under neutral conditions, with the additional advantage of no acid or H_2O_2 addition, as well as its plausible reuse and simple separation due to its magnetic properties.

Keywords: advanced oxidation process; enrofloxacin degradation; photocatalysis; photo-Fenton; wastewater treatment

1. Introduction

Fresh water is a highly valuable resource whose demand is continuously increasing. It is estimated that over the next century, the quantity of available water must increase in the range of 25–60% to satisfy future needs, according to the World Bank 2001 report [1]. Hence, drastic solutions are required in order to ensure future water demands. The possibility of increasing the use of reclaimed water for applications where low-quality water is tolerable seems appealing [2]. A potential use of reclaimed water is agriculture, as it consumes about 70% of global freshwater withdrawals worldwide [3]. However, reused water must also be safe, and for this purpose, a tertiary treatment is necessary in order to eliminate contaminants that cannot be removed by conventional municipal wastewater treatment plants (MWWTPs)—namely, microbiological content and contaminants of emerging concern (CECs), such as antibiotics or pesticides [4–7].

Some parts of southeast Spain are arid lands, but agriculture is among this area's most important economic activities, with a cultivation of a wide range of crops. The combination of water scarcity and high demand for fresh water has forced the use of reclaimed water almost entirely for the total irrigations in the region. In Murcia, for instance, crop irrigation

consumes an average of 110 hm^3/year provided entirely by the 92 MWWTPs located in the community [8–10]. Since CECs can be taken up by crops during their irrigation [11,12], obtaining good quality reclaimed water is an actual target for the region, requiring research on new technologies to be deployed in existing MWWTPs.

Ultraviolet light (UVC) is commonly employed as a tertiary treatment due to its ability to disrupt bacterial DNA and capacity to degrade some organic compounds. However, this treatment is not always enough to completely depurate MWWTP effluents, often leading to the release of by-products [13,14]. Some advanced oxidation processes (AOPs) are based on the use of UVC and are capable of dealing with both microbiological and CEC contents in water [15–17]. These processes have the important practical advantage of being able to be used in the UVC set-ups that are installed at MWWTPs and, on the other hand, they are an environmentally friendly alternative to chlorination, preventing the formation of carcinogenic trihalomethanes [18,19].

The simplest type of AOPs consist of the combination of UVC and H_2O_2 and are based on the ability of UVC to cleave the O-O bond of H_2O_2 to form hydroxyl radicals (·OH). These radicals are among the strongest oxidizing agents and become powerful disinfectants that are also able to degrade most CECs [14,20–22]. In turn, H_2O_2/UVC can be enhanced by the addition of iron salts (photo-Fenton process). This treatment is able to generate highly reactive species upon decomposition of H_2O_2, catalyzed by iron salts [23–25]. However, the photo-Fenton process exhibits its optimum performance under acidic conditions, whereas H_2O_2/UVC is not so pH-dependent, being more effective under basic conditions due to the higher molar absorption coefficient of H_2O_2 at higher pH [20].

An alternative approach is employing heterogeneous photocatalysts (very often, semi-conductors). In this case, the UV irradiation of the semiconductor surface generates an electron-hole couple that leads to the generation of the oxidizing species in aqueous medium able to that degrade CECs [26]. The most widely employed photocatalyst is TiO_2, as it is efficient in disinfection and removal of chemical pollutants, stable, cheap and environmentally friendly [27–30]. However, TiO_2 is not free of inconveniences, some of which are associated with heterogeneous photocatalysis, such as ensuring good contact between catalyst and substrate and, at the same time, an easy removal from the reaction medium after the treatment. In this regard, one promising research line is the use of TiO_2 particles with magnetic cores, to allow separation with magnets and plausible subsequent reuse(s) [31,32]. In this context, FACSA company, in the frame of the Magnox project, has developed a photocatalytic material consisting of a core of SiO_2/Fe_3O_4 coated with TiO_2 [33] with the aim of analyzing its viability for the first time as MWWTP tertiary treatment. Information about the synthesis, characterization, CEC abatement and, reuse of $TiO_2@SiO_2/Fe_3O_4$ and similar photocatalysts can be found elsewhere [34–36].

Inspired by the challenges faced by the aforementioned Spain southeast region (and water-scarcity in general) and the need to incorporate AOP technology in MWWTPs using the previously existing set-ups as much as possible, experiments at the pilot plant scale by using UVC, H_2O_2/UVC, photo-Fenton and heterogeneous photocatalysis with the Magnox material (Magnox/UVC) are reported in this work. Two model compounds have been selected as target: rhodamine-B (RB) has been employed to characterize the system under the different operating conditions; this dye was chosen because it is commonly employed and easy to monitor spectrophotometrically [37–39]. Then, the degradation of enrofloxacin (ENR) was studied under selected conditions. ENR was chosen because it is an antibiotic belonging to the family of fluoroquinolones (considered as CECs), which is frequently found in MWWTPs [40–43].

Finally, the best treatments have been tested with real MWWTP secondary treatment effluent from Alhama de Murcia (Spain) (which treats wastewater coming from an equivalent population of 22,857 inhabitants) managed by FACSA company. Disinfection (elimination of *Escherichia coli* and *Clostridium perfringens*) and effect on physical-chemical parameters—e.g., chemical oxygen demand (COD), total organic carbon (TOC), and transmittance percentage at 254 nm (T_{254}) were monitored, the latter being an indicator of UV

irradiance flux through the treated water; hence, it is related to the proliferation of aquatic microorganisms [44].

2. Materials and Methods

2.1. Reagents

Rhodamine-B, $FeSO_4 \cdot 7H_2O$, H_2O_2 (33% w/v), Na_2SO_3, methanol and acetonitrile were purchased from PanReac-Applichem (Barcelona, Spain). High purity (>99%) enrofloxacin was obtained from Sigma-Aldrich (St. Louis, MO, USA). Formic acid was purchased from VWR Chemicals (Conshohocken, PA, USA) and H_2SO_4 was supplied by Quimivita (Barcelona, Spain). Experiments were performed with tap water (pH = 7.9, total inorganic carbon = 38 mg/L, $[Cl^-]$ = 70 mg/L, $[SO_4^{2-}]$ = 202 mg/L, conductivity = 550 µS/cm), and MWWTP secondary effluent (pH = 7.8, $[Cl^-]$ = 494 mg/L, $[SO_4^{2-}]$ = 483 mg/L, conductivity = 3221 µS/cm, COD = 32 mg/L, TOC = 21 mg/L, 50% T_{254}, *E. coli* 140 CFU/mL and *C. perfringens* spores 5.80 CFU/mL).

Magnox particles were synthetized by employing a suspension of Fe_3O_4 particles (Bayferrox B360 (Lanxess, Cologne, Germany)), colloidal silica (Ludox PT-40 Grace, Columbia, MD, USA) and titania slurry (Aerodisp W740X (Evonik, Essen, Germany)).

In microbiological measurements, Sartorius (Göttingen, Germany) nitrocellulose filters, pore size 0.45 µm, were employed. Lactose TTC Agar/Tergitol 7 culture medium was purchased from VWR Chemicals, and agar TSC was obtained from Scharlau (Barcelona, Spain).

2.2. Photocatalyst Synthesis and Characterization

Magnox particles were synthetized in two steps. First, a suspension of Fe_3O_4 particles in colloidal silica in a relation of 1/20 in weight was spray-dried in a pilot-scale spray-drier (model 00.300, New Tech S.r.l. Italy), obtaining particles with a magnetic core and a silica shell. Afterwards, a suspension of these core–shell particles in a titania slurry was prepared in a relation 1/12 in weight and dried with the same spray-drier. The obtained product consisted of particles with cores of magnetite, transition shells of silica, and surfaces of photocatalytic TiO_2. The as-synthesized particles were calcined at 600 °C for 1 h in a laboratory electric furnace (RHF1600, Carbolite Furnaces Ltd., Sheffield, UK) to sinter the materials and improve their mechanical properties. The obtained particles had a theoretical composition of 1.9 Fe_3O_4, 15.3 SiO_2, and 82.8 TiO_2 (wt.%).

Magnox particles presented a true density of 3.4×10^3 kg/m^3 (measured by a helium stereopycnometer, UPY-10T Ultrapycnometer, Quantachrome Instruments, Boynton Beach, FL, USA) and a specific surface of 59 m^2/g (measured by BET method with a TriStar 3000, Micromeritics Instrument Corp., Norcross, GA, USA). SEM analysis (ESEM Quanta 200, FEI Corp., Hillsboro, OR, USA) estimated a particle size range between 20 and 200 µm (Figure 1A) and confirmed the expected structure of the particles: an internal layer of the mixture magnetite+silica and an external layer of titania (Figure 1B). The central pore is a characteristic of spray-dried materials which can facilitate the fluidization of the particles in the reactor if it is completely closed.

2.3. Chemical and Microbiological Analysis

Decoloration of the solutions containing RB was tracked following the absorbance decay at 552 nm by means of a spectrophotometer (Hach-Lange, Loveland, CO, USA). The same apparatus was employed to determine the transmittance of MWWTP effluent at 254 nm.

ENR concentration was determined with a Hitachi (Tokio, Japan) Chromaster high pressure liquid chromatography (HPLC) coupled with a UV/Vis detector. The column was a Machery-Nagel (Düren, Germany) C18 Nucleodur-π^2 5 µm. The elution was performed in isocratic mode at 0.25 mL/min and the eluent consisted of a mixture formic acid 0.1 M 80% and acetonitrile 20%. The oven was set to 40 °C and the detection was performed at 275 nm.
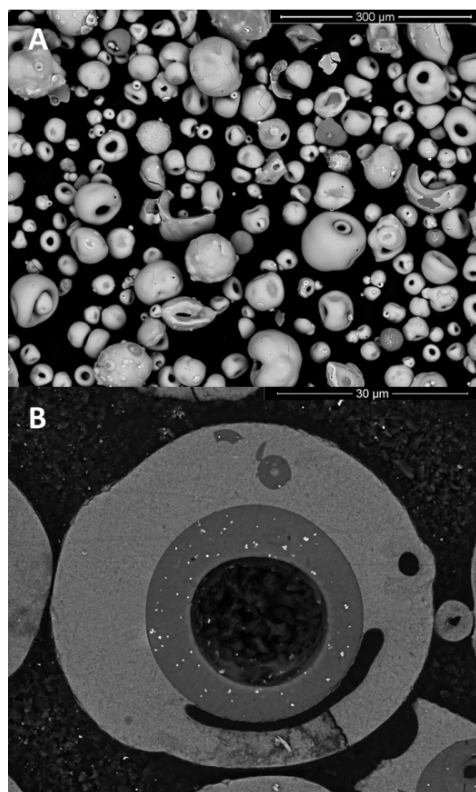
Figure 1. SEM images from Magnox photocatalyst: (**A**) general view of the particles; (**B**) sectioned and polished particle showing the silica (dark layer surrounding the central pore), magnetite (brightest points inside silica layer), and titanium oxide (the grey layer around silica layer).

The degree of mineralization was obtained with the experiments following the decrease in total organic carbon (TOC). These analyses were performed on Shimadzu (Kioto, Japan) TOC-V equipment with a Shimadzu ASI-V autosampler. Chemical oxygen demand (COD) was also monitored using a photometric method (Merck Cell test) and by measuring the resulting color on a Merck Prove 300 photometer. The decay of H_2O_2 concentration in the time-course experiments was measured using MQuant peroxide indicator test strips.

Microbiological analyses were performed employing permanently sterile material. For *E. coli* measurements, 100 mL of MWWTP diluted samples (1:100) were passed through Sartorius (Göttingen, Germany) nitrocellulose filters, with pore sizes of 0.45 μm, which was afterwards placed on a Lactose TTC Agar/Tergitol 7 culture medium. The number of colony formation units (CFUs) was determined after 24 h incubation at 45 °C. *C. perfringens* spore content was determined by Iproma laboratories (Castellón, Spain) based on ISO 14189:2013. The employed methodology consisted of a heat pretreatment at 60 °C for 15 min for inactivation of bacteria in a vegetative state. The samples were filtered afterwards, and the filter was placed on Agar TSC. An incubation in an anaerobiosis generation system at 44 °C for 21 h was performed, measuring the respective CFUs by phosphatase alkaline assay (Sifin) according to ISO 14189.

2.4. Experimental Procedures and Set-Up at Pilot Plant Scale

Experiments with model compounds were performed in tap water at pH 2.8 (employing H_2SO_4 96%) and natural 7.7. The initial concentration of the tested pollutants was 5 mg/L for RB and 25 mg/L in the case of ENR; the latter was only explored at pH 2.8. Pollutant concentrations were high enough to measure mineralization percentages accurately. The described solutions have shown to be stable under dark conditions and air bubbling (30 L/min) for at least 2 h. The H_2O_2/UVC process was studied by employing the stoichiometric amount of H_2O_2 for mineralization of the tested pollutants—25 and

125 mg/L of H_2O_2 for RB and ENR, respectively. This is a useful procedure commonly employed to normalize the amount of hydrogen peroxide added to the reaction medium and to ensure that the process is not stopped because of the exhaustion of this reagent [45]. The same conditions were employed for photo-Fenton experiments (in both studied pHs, 2.8 and natural 7.7), but with the addition of 5 mg/L of Fe(II) added from a stock solution prepared with $FeSO_4 \cdot 7H_2O$, which is a concentration that has been shown to be effective according to previous works [45,46], and it is also the maximum recommended level for treated wastewater according to the FAO [47]. In the experiments involving Magnox, the desired amount of this solid catalyst was added directly into the pilot plant, leaving 10 min before turning on the UVC lamp to ensure complete homogenization.

Experiments were conducted in the reactor pilot plant depicted in Figure 2. In total, 45 L of solution was loaded into a conical vessel with vertical agitation, from the bottom of which the mixture was pumped through a commercial vertical photo-reactor (ATG model UVLA-325-4) equipped with a 325 Watt low-pressure UVC lamp ($\lambda \sim 254$ nm), and recirculated to the conical vessel. The photo-reactor dimensions were: 1.73 m total length, 1.42 m from inlet to outlet, and 175 mm distance between lamp and reactor wall. The employed pumping flow was 400 L/h (level on which the turbulent flux is ensured) in all cases. Samples were taken from an upper tube located at the exit of the photo-reactor. Although Magnox particles presented high densities, the fluidization of the particles in the photoreactor was achieved through fine-adjustment of the air flow rate from the bottom of the column using an air compressor Metabo Basic 250-50 V. This set flow rate was sufficient when the operator visually detected fluidization of the catalyzer along 75% of the length of the column whilst checking that the photocatalyzer was not being washed out from the top of the reactor, with 1.5 L/min air flow being the minimum. In terms of direction, both the air flow and the solution vertically ascended through the photo-reactor.
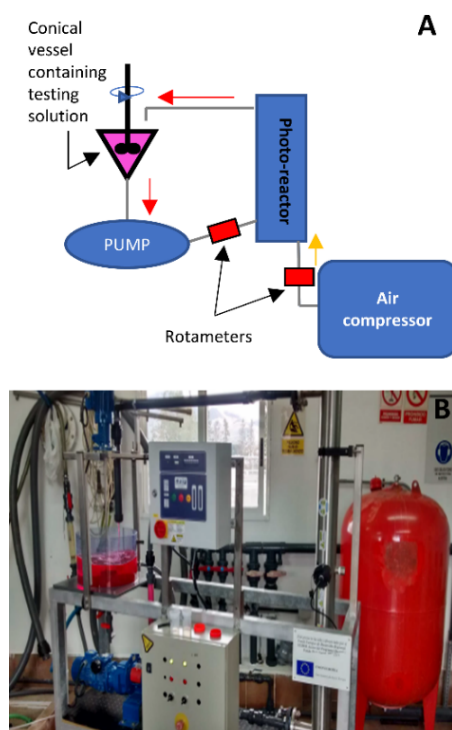

Figure 2. Employed pilot plant: (**A**) scheme and (**B**) picture.

3. Results and Discussion

3.1. Study of the Operational Parameters

A first series of experiments was devoted to determining the effect of Magnox initial concentration (0.5 and 5 g/L) and air flow rate (1.5 and 30 L/min) on the decolorization rate of the RB model dye (Figure 3).
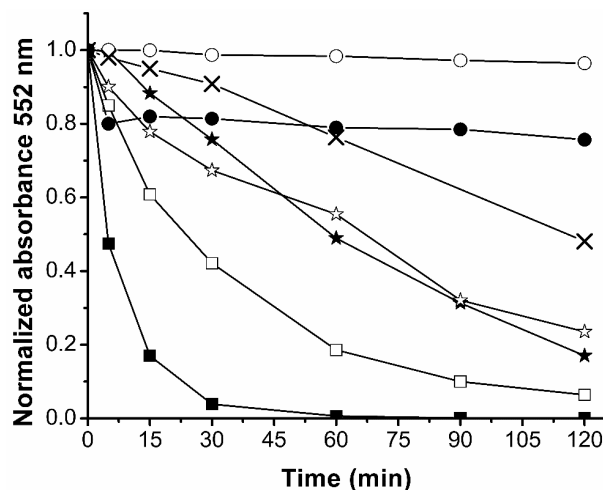

Figure 3. Dye decolorization (rhodamine-B (RB), 5 mg/L) by Magnox/Ultraviolet light (UVC) within different tested operational conditions: dark controls (adsorption) with fixed air flow of 30 L/min, for 0.5 (○) and 5 g/L (●) of photocatalyst; air flow variation with fixed 0.5 g/L of photocatalyst, 1.5 (☆) and 30 L/min (★); air flow variation with fixed 5 g/L of photocatalyst, 1.5 (□) and 30 L/min (■); UVC alone (×) with 30 L/min air flow.

Among the seven experiments performed, the best results were obtained with 5 g/L of Magnox and 30 L/min air flow, as a nearly complete decolouration was reached in about 30 min. Indeed, the best performance observed at the highest air volumetric flow rate was due to the improved suspension of the solid catalyst along the photoreactor. In fact, it was also observed during experiments with 5 g/L of Magnox and 1.5 L/min air flow that the amount of solid during sampling diminished with time, thus indicating that the photocatalyst should be retained within the connections of the pilot plant, or even also inside the photoreactor, losing the material over the course of the experiment due to inadequate mixing. In addition, dark controls have shown that 20% RB absorption on the photocatalyst was also observed when employing the 5 g/L of photocatalyst with an air flow of 30 L/min. This was negligible with the lower tested Magnox amount. Finally, the RB decolorization by photolysis contribution is also shown—ca. 50% in 2 h.

Therefore, we can conclude that when employing higher air flows, in addition to the likelihood of higher reactive oxygen species formation which could have enhanced the overall pollutant abatement [23,48,49], it also increased the availability of the photocatalyst surface to the light and enhanced the mass transfer process through and from the particles. Hence, for the rest of experiments, air flows were 30 L/min. It is important to highlight that the main modifications to the photoreactor could be also taken into account, such as magnetic mixing [50], in order to avoid photocatalyst loss as well as avoiding the use of an air compressor which is expensive.

The efficiency of Magnox was compared with other AOPs that are commonly employed—namely, UVC-photolysis, H_2O_2/UVC, Fenton (Fe(II)/H_2O_2), and photo-Fenton (Fe(II)/H_2O_2/UVC) (Figure 4A). It can be observed that the fastest decolorization was reached with H_2O_2/UVC, followed by Magnox/UVC. Photo-Fenton also enabled fast RB decolorization (100% in 30 min), which was mainly attributed to the H_2O_2/UVC contribution since iron is scarcely able to drive photo-Fenton at the used pH values due to the formation of iron oxides, as has been widely reported [23,51,52]. In line with these

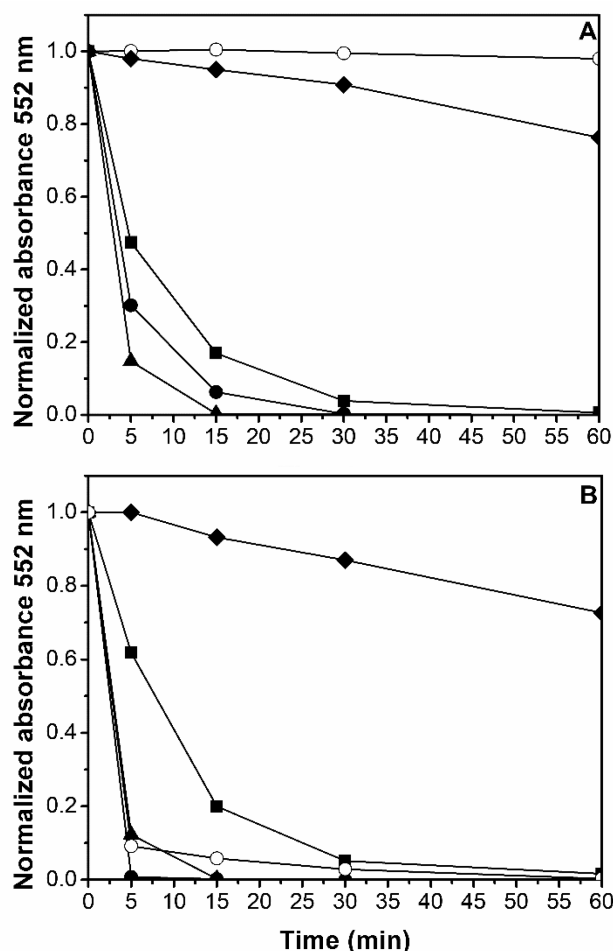statements, in the absence of light, the dark-Fenton process was not able to produce any effect on RB.

Figure 4. Dye decolorization (RB 5 mg/L) profiles with the different studied Advanced Oxidation Processes (AOPs) with air flow of 30 L/min at (**A**) natural pH and (**B**) pH 2.8. Studied processes are represented as follows: UVC (◆), Magnox/UVC (■), H_2O_2/UVC (▲), Fenton (○), and photo-Fenton (●).

Putting all these data together, it can be stated that only H_2O_2/UVC, photo-Fenton and Magnox/UVC were efficient under the studied operational conditions. However, changing some parameters (e.g., pH) might result in a dramatic change in these conclusions (Figure 4B). For instance, photo-Fenton at pH = 2.8, which is the optimal value for this process [53], was able to completely decolorize the solution in 5 min, while 90% decrease in the absorbance was reached for dark-Fenton under the same conditions. On the other hand, pH had no significant effect on the UVC, Magnox/UVC or H_2O_2/UVC processes.

3.2. Enrofloxacin Removal and Mineralization

In order to gain further insight into the efficiency of each AOP studied on the degradation of a more complex pollutant commonly found in real effluents, ENR was chosen as a target compound. This product is a widely employed antibiotic that belongs to the family of fluoroquinolones [40,54] and, furthermore, its photo-Fenton degradation has been recently studied by the authors [55].

The ENR removal experiments were performed at an initial pH of 2.8, a condition where all the tested AOPs have shown the best RB decolorization rates (Figure 4B), employing an air flow rate of 30 L/min (Figure 5A). In coincidence with RB degradations at acidic conditions, ENR presented fast total removals with all the tested AOPs. Fenton and photo-Fenton were very efficient in ENR removal, but the combination of H_2O_2/UVC was

also able to completely abate this antibiotic in 15 min. In the case of Magnox/UVC, even though the reaction was notably slower than the ones employing hydrogen peroxide, ENR removal was still faster than with UVC alone, thus demonstrating again the photocatalytic activity of the material.
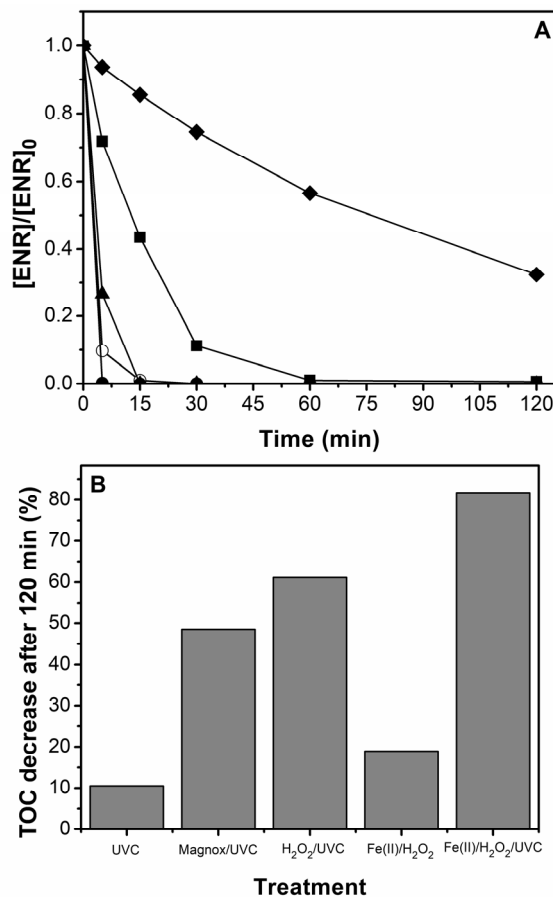

Figure 5. Enrofloxacin (ENR) 25 mg/L removals at pH 2.8 with air flow of 30 L/min. (**A**): UVC (◆), Magnox/UVC (■), H_2O_2/UVC (▲), Fenton (○), and photo-Fenton (●); (**B**) mineralization percentages.

Mineralization of ENR was also followed and some interesting variations in the trends were observed: high degree of mineralization (above 50% after 120 min) was reached for the three processes following the rates trend: photo-Fenton > H_2O_2/UVC > Magnox/UVC (Figure 5B). On the other hand, the decrease in TOC for Fenton and UVC was much lower (below 20% after 120 min).

3.3. Magnox/UVC Influence on MWWTP Water

Having already studied the CEC removal efficiency of Magnox/UVC, in order to gain further insight into the real applicability of the Magnox/UVC process, the best operating conditions previously selected were applied to MWWTP secondary treatment effluent. In this way, we can analyze the behavior of the water matrix with the photocatalyst so the combination of trace amounts of CECs in MWWTP water could be better explained in further studies.

In these experiments, the concentration of Magnox was 5 g/L and the pump and air flows were fixed at 400 L/h and 30 L/min, respectively. Five parameters were chosen to track the effect of the treatment: a physical parameter—(i) transmittance; two chemical gross parameters related to the presence of organic matter—namely, (ii) COD and (iii) TOC; the CFUs of two relevant microbiological species—(iv) *Escherichia coli* and (v) *Clostridium perfringens*. UVC irradiation in the absence of Magnox was also tested. As a summary, the results obtained after 120 min of treatment are shown in Table 1. It can be

observed that 120 min of irradiation was able to reach full bacteria content inactivation with and without Magnox, thus showing that UVC is powerful enough to disinfect the studied water. However, differences among both methods can be observed in the other assessed parameters. In this case, none of the employed technologies were able to yield complete removal of the organic matter, although better results were reached with the Magnox/UVC.

Table 1. UVC and Magnox/UVC tertiary treatment comparison.

Parameter	Initial Value	After 120 min UVC		After 120 min Magnox/UVC	
		Final Value	Increase/Decrease Percentage	Final Value	Increase/Decrease Percentage
Transmittance 254 nm (T_{254}) (%)	50	73	46	86	72
COD (mg/L)	32	27	14	24	24
TOC (mg/L)	21	17	20	14	33
E. coli (CFU/mL)	140	0	100	0	100
C. perfringens spores (CFU/mL)	5.8	0	100	0	100

4. Conclusions

Pollutant abatement and wastewater tertiary treatment were tested with direct irradiation of UVC light and AOPs at the pilot plant scale. At neutral pH, faster decolorization of RB was observed in H_2O_2/UVC > photo-Fenton > Magnox/UVC > UVC, and was negligible when using dark-Fenton. However, as expected, when setting acidic conditions, a large enhancement of degradation rate was observed with Fenton and photo-Fenton processes, attaining fast total RB decolorization in 60 and 5 min, respectively.

When analyzing ENR degradation at pH 2.8, the photo-Fenton process proved to be the most efficient tertiary treatment by means of pollutant removal and mineralization. However, it should be highlighted that realistic treatment conditions included the development of the reactions at circumneutral pH, and therefore H_2O_2/UVC becomes the best option.

Although obtained results with Magnox/UVC were slower than H_2O_2/UVC and photo-Fenton, the advantage of its employment at neutral pH is shown to be effective. Additionally, since Magnox/UVC has the additional advantage of no acid or H_2O_2 addition, as well as its plausible reusability and simple separation due to its magnetic properties, further research on photocatalyst homogenization inside the reactor is required, with the possibility of Magnox/UVC being more efficient than H_2O_2/UVC; hence, it is also more cost-effective than the latter.

Finally, successful complete inactivation of bacteria was attained when applying UVC, with no need for the addition of Magnox, as a tertiary treatment after 120 min. However, COD and TOC decreases were faster when combining UVC with the photocatalyst, also observing a faster T_{254} increase.

The optimization of operational conditions, including an economical study for Magnox/UVC, toxicity assays, iron lixiviation and its employment for CEC degradation in a more realistic situation (concentration and water matrix), is certainly needed. Since the effect of the process against pollutant abatement and MWWTP water alone, respectively, had been now studied, its application to CEC in lower concentrations (i.e., µg/L) in the MWWTP wastewater will be the next step.

Author Contributions: Conceptualization, I.S., F.V. and A.A.; investigation, I.S. and S.M.; resources, A.A., S.M., J.C. and F.V.; writing—original draft preparation, I.S.; writing—review and editing, I.S., C.E.-O., I.O. and A.A.; visualization, I.S. and A.A.; supervision, C.E.-O., I.O. and A.A.; project administration, C.E.-O., I.O. and A.A.; funding acquisition, J.C., F.V., C.E.-O., I.O. and A.A. All authors have read and agreed to the published version of the manuscript.

References

1. World Bank. *The World Bank Annual Report 2001: Volume 1*; Year in Review; World Bank: Washington, DC, USA, 2001; Available online: https://openknowledge.worldbank.org/handle/10986/13933 (accessed on 22 May 2020).

2. Asano, T.; Maeda, M.; Takaki, M. Wastewater reclamation and reuse in Japan: Overview and implementation examples. *Water Sci. Technol.* **1996**, *34*, 219–226. [CrossRef]

3. Intriago, J.C.; López-Gálvez, F.; Allende, A.; Vivaldi, G.A.; Camposeo, S.; Nicolás Nicolás, E.; Alarcón, J.J.; Pedrero Salcedo, F. Agricultural reuse of municipal wastewater through an integral water reclamation management. *J. Environ. Manag.* **2018**, *213*, 135–141. [CrossRef] [PubMed]

4. Levine, A.D.; Asano, T. Peer Reviewed: Recovering Sustainable Water from Wastewater. *Environ. Sci. Technol.* **2004**, *38*, 201A–208A. [CrossRef] [PubMed]

5. Salimi, M.; Esrafili, A.; Gholami, M.; Jafari, A.J.; Kalantary, R.R.; Farzadkia, M.; Kermani, M.; Sobhi, H.R. Contaminants of emerging concern: A review of new approach in AOP technologies. *Environ. Monit. Assess.* **2017**, *189*. [CrossRef]

6. Xu, J.; Wu, L.; Chang, A.C. Degradation and adsorption of selected pharmaceuticals and personal care products (PPCPs) in agricultural soils. *Chemosphere* **2009**, *77*, 1299–1305. [CrossRef]

7. Lyu, S.; Chen, W.; Zhang, W.; Fan, Y.; Jiao, W. Wastewater reclamation and reuse in China: Opportunities and challenges. *J. Environ. Sci.* **2016**, *39*, 86–96. [CrossRef]

8. Maestre-Valero, J.F.; Gonzalez-Ortega, M.J.; Martinez-Alvarez, V.; Gallego-Elvira, B.; Conesa-Jodar, F.J.; Martin-Gorriz, B. Revaluing the nutrition potential of reclaimed water for irrigation in southeastern Spain. *Agric. Water Manag.* **2019**, *218*, 174–181. [CrossRef]

9. Acosta, J.A.; Faz, A.; Jansen, B.; Kalbitz, K.; Martínez-Martínez, S. Assessment of salinity status in intensively cultivated soils under semiarid climate, Murcia, SE Spain. *J. Arid Environ.* **2011**, *75*, 1056–1066. [CrossRef]

10. Fleskens, L.; Nainggolan, D.; Termansen, M.; Hubacek, K.; Reed, M.S. Regional consequences of the way land users respond to future water availability in Murcia, Spain. *Reg. Environ. Chang.* **2013**, *13*, 615–632. [CrossRef]

11. Calderón-Preciado, D.; Matamoros, V.; Bayona, J.M. Occurrence and potential crop uptake of emerging contaminants and related compounds in an agricultural irrigation network. *Sci. Total Environ.* **2011**, *412–413*, 14–19. [CrossRef]

12. Christou, A.; Papadavid, G.; Dalias, P.; Fotopoulos, V.; Michael, C.; Bayona, J.M.; Piña, B.; Fatta-Kassinos, D. Ranking of crop plants according to their potential to uptake and accumulate contaminants of emerging concern. *Environ. Res.* **2019**, *170*, 422–432. [CrossRef]

13. Sun, Y.; Cho, D.W.; Graham, N.J.D.; Hou, D.; Yip, A.C.K.; Khan, E.; Song, H.; Li, Y.; Tsang, D.C.W. Degradation of antibiotics by modified vacuum-UV based processes: Mechanistic consequences of H_2O_2 and $K_2S_2O_8$ in the presence of halide ions. *Sci. Total Environ.* **2019**, *664*, 312–321. [CrossRef] [PubMed]

14. Yin, K.; Deng, L.; Luo, J.; Crittenden, J.; Liu, C.; Wei, Y.; Wang, L. Destruction of phenicol antibiotics using the UV/H_2O_2 process: Kinetics, byproducts, toxicity evaluation and trichloromethane formation potential. *Chem. Eng. J.* **2018**, *351*, 867–877. [CrossRef]

15. Pera-Titus, M.; García-Molina, V.; Baños, M.A.; Giménez, J.; Esplugas, S. Degradation of chlorophenols by means of advanced oxidation processes: A general review. *Appl. Catal. B Environ.* **2004**, *47*, 219–256. [CrossRef]

16. Malato, S.; Fernández-Ibáñez, P.; Maldonado, M.I.; Blanco, J.; Gernjak, W. Decontamination and disinfection of water by solar photocatalysis: Recent overview and trends. *Catal. Today* **2009**, *147*, 1–59. [CrossRef]

17. Bernabeu, A.; Vercher, R.F.; Santos-Juanes, L.; Simón, P.J.; Lardín, C.; Martínez, M.A.; Vicente, J.A.; González, R.; Llosá, C.; Arques, A.; et al. Solar photocatalysis as a tertiary treatment to remove emerging pollutants from wastewater treatment plant effluents. *Catal. Today* **2011**, *161*, 235–240. [CrossRef]

18. Matamoros, V.; Mujeriego, R.; Bayona, J.M. Trihalomethane occurrence in chlorinated reclaimed water at full-scale wastewater treatment plants in NE Spain. *Water Res.* **2007**, *41*, 3337–3344. [CrossRef]

19. World Health Organization. *Trihalomethanes in Drinking-Water Background Document for Development of WHO Guidelines for Drinking-Water Quality*; World Health Organization: Geneva, Switzerland, 2005.

20. Legrini, O.; Oliveros, E.; Braun, A.M. Photochemical Processes for Water Treatment. *Chem. Rev.* **1993**, *93*, 671–698. [CrossRef]

21. Lee, Y.; Gerrity, D.; Lee, M.; Gamage, S.; Pisarenko, A.; Trenholm, R.A.; Canonica, S.; Snyder, S.A.; Von Gunten, U. Organic Contaminant Abatement in Reclaimed Water by UV/H_2O_2 and a Combined Process Consisting of O_3/H_2O_2 Followed by UV/H_2O_2: Prediction of Abatement Efficiency, Energy Consumption, and Byproduct Formation. *Environ. Sci. Technol.* **2016**, *50*, 3809–3819. [CrossRef]

22. Jung, Y.J.; Kim, W.G.; Yoon, Y.; Kang, J.W.; Hong, Y.M.; Kim, H.W. Removal of amoxicillin by UV and UV/H_2O_2 processes. *Sci. Total Environ.* **2012**, *420*, 160–167. [CrossRef]

23. Pignatello, J.J.; Oliveros, E.; MacKay, A. Advanced Oxidation Processes for Organic Contaminant Destruction Based on the Fenton Reaction and Related Chemistry. *Crit. Rev. Environ. Sci. Technol.* **2006**, *36*, 1–84. [CrossRef]

24. Amat, A.M.; Arques, A.; Miranda, M.A.; Seguí, S. Photo-fenton reaction for the abatement of commercial surfactants in a solar pilot plant. *Sol. Energy* **2004**, *77*, 559–566. [CrossRef]
25. Prevot, A.B.; Baino, F.; Fabbri, D.; Franzoso, F.; Magnacca, G.; Nisticò, R.; Arques, A. Urban biowaste-derived sensitizing materials for caffeine photodegradation. *Environ. Sci. Pollut. Res.* **2017**, *24*, 12599–12607. [CrossRef] [PubMed]
26. Fujishima, A.; Rao, T.N.; Tryk, D.A. Titanium dioxide photocatalysis. *J. Photochem. Photobiol. C Photochem. Rev.* **2000**, *1*, 1–21. [CrossRef]
27. Zhang, Z.; Wang, C.C.; Zakaria, R.; Ying, J.Y. Role of particle size in nanocrystalline TiOi-based photocatalysts. *J. Phys. Chem. B* **1998**, *102*, 10871–10878. [CrossRef]
28. Calza, P.; Sakkas, V.A.; Medana, C.; Baiocchi, C.; Dimou, A.; Pelizzetti, E.; Albanis, T. Photocatalytic degradation study of diclofenac over aqueous TiO_2 suspensions. *Appl. Catal. B Environ.* **2006**, *67*, 197–205. [CrossRef]
29. Henderson, M.A. A surface science perspective on TiO_2 photocatalysis. *Surf. Sci. Rep.* **2011**, *66*, 185–297. [CrossRef]
30. Liu, G.; Wang, L.; Yang, H.G.; Cheng, H.M.; Lu, G.Q. Titania-based photocatalysts—Crystal growth, doping and heterostructuring. *J. Mater. Chem.* **2010**, *20*, 831–843. [CrossRef]
31. Polliotto, V.; Pomilla, F.R.; Maurino, V.; Marcì, G.; Prevot, A.B.; Nisticò, R.; Magnacca, G.; Paganini, M.C.; Robles, L.P.; Perez, L.; et al. Different approaches for the solar photocatalytic removal of micro-contaminants from aqueous environment: Titania vs. hybrid magnetic iron oxides. *Catal. Today* **2019**, *328*, 164–171. [CrossRef]
32. Nisticò, R.; Celi, L.R.; Prevot, A.B.; Carlos, L.; Magnacca, G.; Zanzo, E.; Martin, M. Sustainable magnet-responsive nanomaterials for the removal of arsenic from contaminated water. *J. Hazard. Mater.* **2018**, *342*, 260–269. [CrossRef]
33. García, C.D.; Bermejo, J.T.G.; Tragstaec, C.G.; Tunc, I.; Rogel, J.A.; Sanchez, J.J.M. Uso de biorreactores con madera para desnitrificación de salmueras en el campo de cartagena. In Proceedings of the Congreso Internacional de Aedyr, Toledo, Spain, 23–25 October 2018.
34. Gad-Allah, T.A.; Fujimura, K.; Kato, S.; Satokawa, S.; Kojima, T. Preparation and characterization of magnetically separable photocatalyst ($TiO_2/SiO_2/Fe_3O_4$): Effect of carbon coating and calcination temperature. *J. Hazard. Mater.* **2008**, *154*, 572–577. [CrossRef] [PubMed]
35. Wang, R.; Wang, X.; Xi, X.; Hu, R.; Jiang, G. Preparation and photocatalytic activity of magnetic $Fe_3O_4/SiO_2/TiO_2$ composites. *Adv. Mater. Sci. Eng.* **2012**, *2012*. [CrossRef]
36. Chen, X.Q.; Zhang, H.X.; Shen, W.H. Preparation and characterization of the magnetic $Fe_3O_4@TiO_2$ nanocomposite with the in-situ synthesis coating method. *Mater. Chem. Phys.* **2018**, *216*, 496–501. [CrossRef]
37. Daneshvar, N.; Behnajady, M.A.; Mohammadi, M.K.A.; Dorraji, M.S.S. UV/H_2O_2 treatment of Rhodamine B in aqueous solution: Influence of operational parameters and kinetic modeling. *Desalination* **2008**, *230*, 16–26. [CrossRef]
38. Kansal, S.K.; Singh, M.; Sud, D. Studies on photodegradation of two commercial dyes in aqueous phase using different photocatalysts. *J. Hazard. Mater.* **2007**, *141*, 581–590. [CrossRef] [PubMed]
39. Zhao, J.; Wu, T.; Wu, K.; Oikawa, K.; Hidaka, H.; Serpone, N. Photoassisted degradation of dye pollutants. 3. Degradation of the cationic dye rhodamine B in aqueous anionic surfactant/TiO_2 dispersions under visible light irradiation: Evidence for the need of substrate adsorption on TiO_2 particles. *Environ. Sci. Technol.* **1998**, *32*, 2394–2400. [CrossRef]
40. Van Doorslaer, X.; Dewulf, J.; Van Langenhove, H.; Demeestere, K. Fluoroquinolone antibiotics: An emerging class of environmental micropollutants. *Sci. Total Environ.* **2014**, *500–501*, 250–269. [CrossRef]
41. Rutgersson, C.; Fick, J.; Marathe, N.; Kristiansson, E.; Janzon, A.; Angelin, M.; Johansson, A.; Shouche, Y.; Flach, C.F.; Larsson, D.G.J. Fluoroquinolones and qnr genes in sediment, water, soil, and human fecal flora in an environment polluted by manufacturing discharges. *Environ. Sci. Technol.* **2014**, *48*, 7825–7832. [CrossRef]
42. de los Ángeles Bernal-Romero, M.; Boluda-Botella, N.; Rico, D.P. Removal of emerging pollutants in water treatment plants: Adsorption of methyl and propylparaben onto powdered activated carbon. *Adsorption* **2019**, *25*, 983–999. [CrossRef]
43. Speltini, A.; Sturini, M.; Maraschi, F.; Mandelli, E.; Vadivel, D.; Dondi, D.; Profumo, A. Preparation of silica-supported carbon by Kraft lignin pyrolysis, and its use in solid-phase extraction of fluoroquinolones from environmental waters. *Microchim. Acta* **2016**, *183*, 2241–2249. [CrossRef]
44. Mostofa, K.M.G.; Liu, C.; Mottaleb, M.A.; Wan, G.; Ogawa, H.; Vione, D.; Yoshioka, T.; Wu, F. Dissolved Organic Matter in Natural Waters. In *Biogeochemistry*; Mostofa, K.M.G., Yoshioka, T., Mottaleb, A., Vione, D., Eds.; Environmental Science and Engineering; Springer: Berlin/Heidelberg, Germany, 2013; Volume 179, pp. 1–137. ISBN 978-3-642-32222-8.
45. Gomis, J.; Gonçalves, M.G.; Vercher, R.F.; Sabater, C.; Castillo, M.A.; Prevot, A.B.; Amat, A.M.; Arques, A. Determination of photostability, biocompatibility and efficiency as photo-Fenton auxiliaries of three different types of soluble bio-based substances (SBO). *Catal. Today* **2015**, *252*, 177–183. [CrossRef]
46. García-Ballesteros, S.; Mora, M.; Vicente, R.; Sabater, C.; Castillo, M.A.; Arques, A.; Amat, A.M. Gaining further insight into photo-Fenton treatment of phenolic compounds commonly found in food processing industry. *Chem. Eng. J.* **2016**, *288*, 126–136. [CrossRef]
47. Ayers, R.S.; Westcot, D.W. Water Quality for Agriculture. Available online: http://www.fao.org/3/t0234e/t0234e00.htm (accessed on 22 May 2020).
48. Wang, L.; Ali, J.; Wang, Z.; Oladoja, N.A.; Cheng, R.; Zhang, C.; Mailhot, G.; Pan, G. Oxygen nanobubbles enhanced photodegradation of oxytetracycline under visible light: Synergistic effect and mechanism. *Chem. Eng. J.* **2020**, *388*, 124227. [CrossRef]

49. Haddou, M.; Benoit-Marquié, F.; Maurette, M.-T.; Oliveros, E. Oxidative Degradation of 2,4-Dihydroxybenzoic Acid by the Fenton and Photo-Fenton Processes: Kinetics, Mechanisms, and Evidence for the Substitution of H_2O_2 by O_2. *Helv. Chim. Acta* **2010**, *93*, 1067–1080. [CrossRef]

50. Kostedt IV, W.L.; Drwiega, J.; Mazyck, D.W.; Lee, S.W.; Sigmund, W.; Wu, C.Y.; Chadik, P. Magnetically agitated photocatalytic reactor for photocatalytic oxidation of aqueous phase organic pollutants. *Environ. Sci. Technol.* **2005**, *39*, 8052–8056. [CrossRef] [PubMed]

51. Stefánsson, A. Iron(III) hydrolysis and solubility at 25 °C. *Environ. Sci. Technol.* **2007**, *41*, 6117–6123. [CrossRef] [PubMed]

52. Pignatello, J.J. Dark and Photo Assisted Fe^{3+} Catalyzed Degradation of Chlorophenoxy Herbicides by Hydrogen Peroxide. *Environ. Sci. Technol* **1992**, *26*, 944–951. [CrossRef]

53. Santos-Juanes, L.; Amat, A.A.; Arques, A. Strategies to Drive Photo-Fenton Process at Mild Conditions for the Removal of Xenobiotics from Aqueous Systems. *Curr. Org. Chem.* **2017**, *21*, 1074–1083. [CrossRef]

54. Liu, S.; Dong, G.; Zhao, H.; Chen, M.; Quan, W.; Qu, B. Occurrence and risk assessment of fluoroquinolones and tetracyclines in cultured fish from a coastal region of northern China. *Environ. Sci. Pollut. Res.* **2018**, *25*, 8035–8043. [CrossRef]

55. Sciscenko, I.; Garcia-Ballesteros, S.; Sabater, C.; Castillo, M.A.; Escudero-Oñate, C.; Oller, I.; Arques, A. Monitoring photolysis and (solar photo)-Fenton of enrofloxacin by a methodology involving EEM-PARAFAC and bioassays: Role of pH and water matrix. *Sci. Total Environ.* **2020**, *719*, 137331. [CrossRef]